3

Tectonics and Seismicity

A. F. Espinosa, U.S. Geological Survey, Denver, Colorado
M. L. Hall, Escuela Politécnica Nacional, Quito, Ecuador
H. Yepes, Escuela Politécnica Nacional, Quito, Ecuador

INTRODUCTION

Ecuador is exposed continually to earthquakes and other geologic hazards. In particular, earthquake potential has always been a threat to the inhabitants of Ecuador, so that coexisting with earthquake activity has become part of the Ecuadorian culture.

From the hazards point of view, one must differentiate between earthquakes of tectonic origin and those associated with volcanism. In the past 80 years several large earthquakes (interplate events) have occurred in Ecuador's subduction zone, and their rupture mechanisms were varied (Kanamori and McNally, 1982). Shallow intraplate events, such as the March 1987 earthquakes, occur in the Andes, distant from the active subduction zone. These earthquakes created a serious socioeconomic problem for the country and triggered hundreds of associated geologic hazards—massive landslides, subsidence, liquefaction, impoundment of rivers, and other effects common to earthquakes that have occurred in similar geologic settings (Espinosa, 1979).

Although several destructive intraplate earthquakes have occurred, no systematic probabilistic studies have been done to ascertain the earthquake hazard. Using macroseismic information from chronicles of the sixteenth century (Egred, 1988), an approximate epicenter at 0.14°S and 78.27°W was assigned to an earthquake that took place in April 1541 with a magnitude of 7.0. On August 16, 1868, a great earthquake occurred at 0.31°N and 78.18°W with a magnitude of 7.7. On June 23, 1925, a magnitude 6.8 earthquake with a depth of focus of 180 km occurred and was located at 0.0°, 77°W. A great interplate earthquake with an M_w = 8.8 took place on January 31, 1906, with a length of rupture on the order of 500 km (Kanamori and McNally, 1982). Other large interplate earthquakes have occurred in north-

western Ecuador, including those of May 14, 1942 (M_s = 7.9) and January 19, 1958 (M_s = 7.8). The March 5, 1987,[1], main event (M_s = 6.9) occurred in interior Ecuador, in a highly faulted zone of Jurassic intrusive and Cretaceous metamorphic rocks. This earthquake and its largest foreshock (M_s = 6.1) are the subject of this chapter.

TECTONIC SETTING

Active seismicity occurs continuously for more than 6,000 km along the western edge of South America. The oceanic Nazca Plate is steadily being subducted eastward under the continent along a well-defined Wadati-Benioff zone. The most tectonically notable feature of the South American Plate is the Andean Mountains, which share a common tectonic pattern from Colombia in the N to southern Chile. The major physiographic features of the Andes are the result of the subduction of the Pacific lithosphere beneath the South American continent.

Three distinct tectonic regimes characterize the Nazca Plate oceanward of Colombia and Ecuador. Between latitudes 1 and 7°N, the ocean bottom physiography is nearly flat. Its age varies progressively from 10 to 26 million years toward the N (Lonsdale and Klitgard, 1978); its subduction to the E, under Colombia, coincides with a row of active stratovolcanoes. Between latitudes 2 and 4°S, the ocean bottom in front of the Ecuadorian Trench is a fractured and complex zone, 230 km wide. This region is cut by several oceanic fracture zones with NE-trending directions, identified as the Grijalva, Alvarado, and Sarmiento fractures. As this region is subducted under the South American continent, it may behave as a separate microplate independent of the adjacent plates (Pennington, 1981; Hall and Wood, 1985).

In between these two tectonic regimes, between latitude 1°N and 2°S, a submarine mountain range called the Carnegie Ridge, which was generated by the Galapagos mantle plume, collides against the South American continent. This mountain range is approximately 300 km wide and 3 km high, and rests upon older oceanic crust more than 16 million years old. During the past 25 million years, the Nazca Plate has moved eastward at a relative plate velocity of 5 cm/yr (Pilger, 1983), subducting the E-W- oriented Carnegie Ridge under central Ecuador. Lonsdale (1978) estimated that the subduction of the Carnegie Ridge started about 2 or 3 million years ago, while Pennington (1981) estimated an even earlier beginning. Probably its subduction began 5 to 6 million years ago, when, because of the

[1]Times and dates in this chapter are based on local Ecuadorian time except where specifically noted as being U.T.C. (Universal Time Coordinate), which is equivalent to Greenwich Mean Time.

difficulty in subducting this large physiographic feature, the Nazca Plate's eastward journey slowed, which finally permitted the uniform lava emission from the Galapagos plume to build subaerial volcanoes before the plate moved onward (J. W. Spence and M. L. Hall, personal communication, 1987).

Where the subduction of the Carnegie Ridge takes place, the trench is shallow, the coastal region is being uplifted, and extensive and chemically diverse volcanism occurs in the Andes. The mode of faulting and seismicity of the region may be related to the subduction of the Carnegie Ridge. Other tectonic features can also be attributed to this subduction, such as the greater height of the Ecuadorian Andes in this zone, the formation of stratovolcanoes, and active strike-slip faults (Hall and Wood, 1985). The Yaquina fracture zone (Lonsdale and Klitgard, 1978) is not parallel to adjacent N-S trending transform faults in the Panama Basin, but swings westward as it approaches the Carnegie Ridge, suggesting that the subduction of the Nazca Plate in this region is being slowed considerably, most probably because of the difficulty in subducting a very large physiographic feature such as the Carnegie Ridge (Hall and Wood, 1985). The collision of the Carnegie Ridge with continental Ecuador has altered the tectonic stress distribution along this convergent margin, resulting in the creation of numerous faults with NW-SE and NE-SW trends. Well-known fault systems oriented NE-SW include those of the Gulf of Guayaquil, La Pallatanga, and the Alausi-Guamote Valley faults, among others. Several of the destructive earthquakes that have occurred in Ecuador, the Riobamba in 1797 and the Alausi in 1961, among others, have been correlated with these NE-SW trending faults. Major lineaments and faults with NW-SE orientations have been identified by Hall and Wood (1985) as delimiting regions of tectonic segmentation, the most important ones being the Esmeraldas-Pastaza and the Rio Mira-Salado lineaments. The intersection of several sets of conjugate faults occurs in the Inter-Andean Valley, a region well known for its high seismicity and destructive earthquakes, such as the Ibarra earthquake of 1868, the Ambato earthquake of 1949, and the Pastocalle earthquakes of 1944 and 1976.

In the region of the March 5, 1987, earthquake, four principal sets of faults and lineaments have been clearly identified on satellite images (LANDSAT No. 010060; unpublished identification and interpretation by M. L. Hall, 1986) as shown in Figure 3.1. The Abra fault trends N40°E and passes through the western foot of Reventador Volcano (Figure 3.1). This fault has a surface expression of at least 180 km in length, as identified from the LANDSAT images. Parallel lineaments with a length of up to 80 km are visible about 10 km to the NW from the first fault. Another fault lying E of Reventador Volcano and trending parallel to the above faults is known as the Rio Quijos fault (Figure 3.1). These faults are all considered

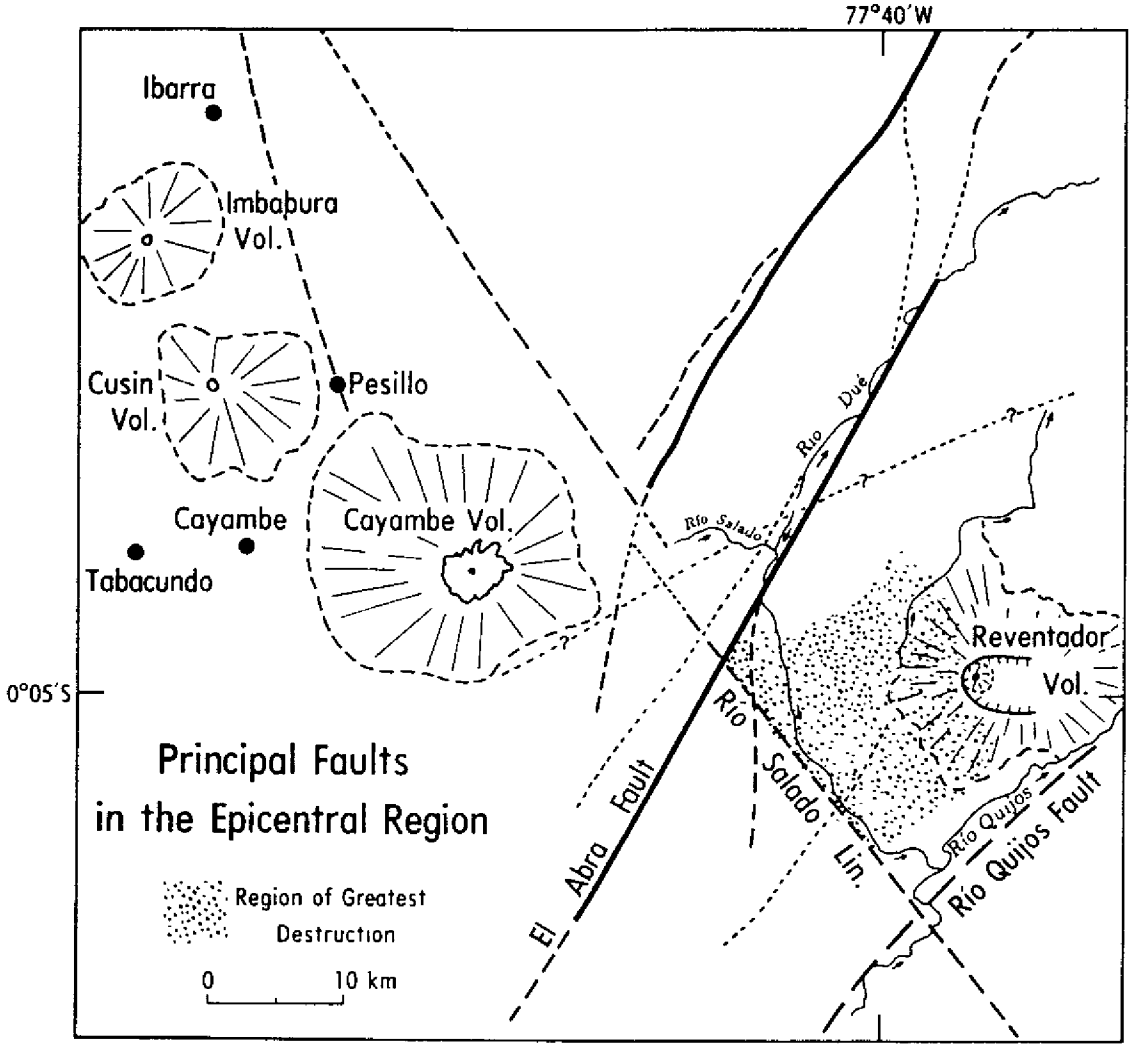

FIGURE 3.1 Map showing the fault systems around the epicentral region (LANDSAT imagery No. 010060, unpublished identification and interpretation by M. L. Hall, 1986).

to be steep reverse faults. The fourth system is associated with the Rio Mira-Salado lineament; this system trends N29°W and is 260 km long. Some of these tectonic features are also shown in Figure 3.2, along with the location of Reventador Volcano.

SEISMICITY AND FOCAL MECHANISMS

The shallow seismicity of the region from latitude 5°S to 5°N and longitude 75° to 85°W, for the time period from 1962 through 1987, is shown in Figure 3.3A. In this figure all the instrumentally recorded shallow earthquakes with uncertain depths are assigned depths of 33 km; these are likely to be shallow, as depth phases are not well separated. Earthquakes with

body- and/or surface-wave magnitudes equal to or greater than 4.5 are plotted. The highest seismicity in this figure occurs in the Ecuador-Colombia zone from latitude 1 to 4°N and longitude 77 to 80°W, most of which are aftershocks following the December 12, 1979, (M_s = 7.7) earthquake. There is also a diffuse seismic zone in the interior of Ecuador that shows no definitive pattern that can be directly associated with the regional tectonic structures at this scale. The earthquake distributions for depths of focus between 33 and 100 km, and between 100 and 300 km, respectively, are shown in Figures 3.3B and 3.3C. The seismic activity portrayed in Figure 3.3B shows a concentration of maximum seismicity in the SW part of Ecuador. The lithosphere in the N part of the Nazca Plate has a gentle angle of subduction, and its geometrical configuration is not uniform, because of the presence of the subducting Carnegie Ridge. The highest seismicity at depths greater than 100 km is shown in Figure 3.3C and is concentrated between latitude 1 and 2°S and at approximately longitude 78°W. The damaging earthquakes of historic times have been large, shallow earthquakes whose epicenters were near urban areas.

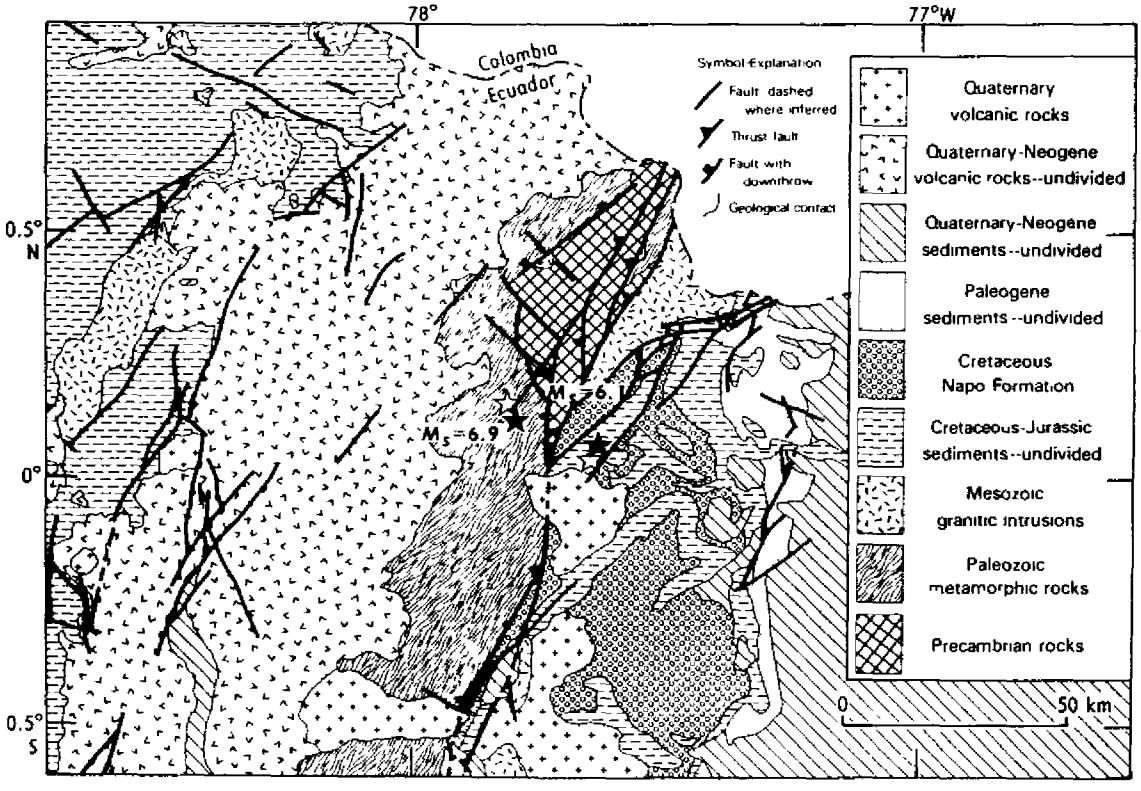

FIGURE 3.2 Map showing the major fault systems in and around the epicentral region. Also shown are the major geological units and the epicenter locations for the main event (M_s = 6.9) and of the main foreshock (M_s = 6.1) as solid stars and their relocated epicenters as open stars. Their earthquake hypocentral parameters are listed in Tables 3.1 and 3.2.

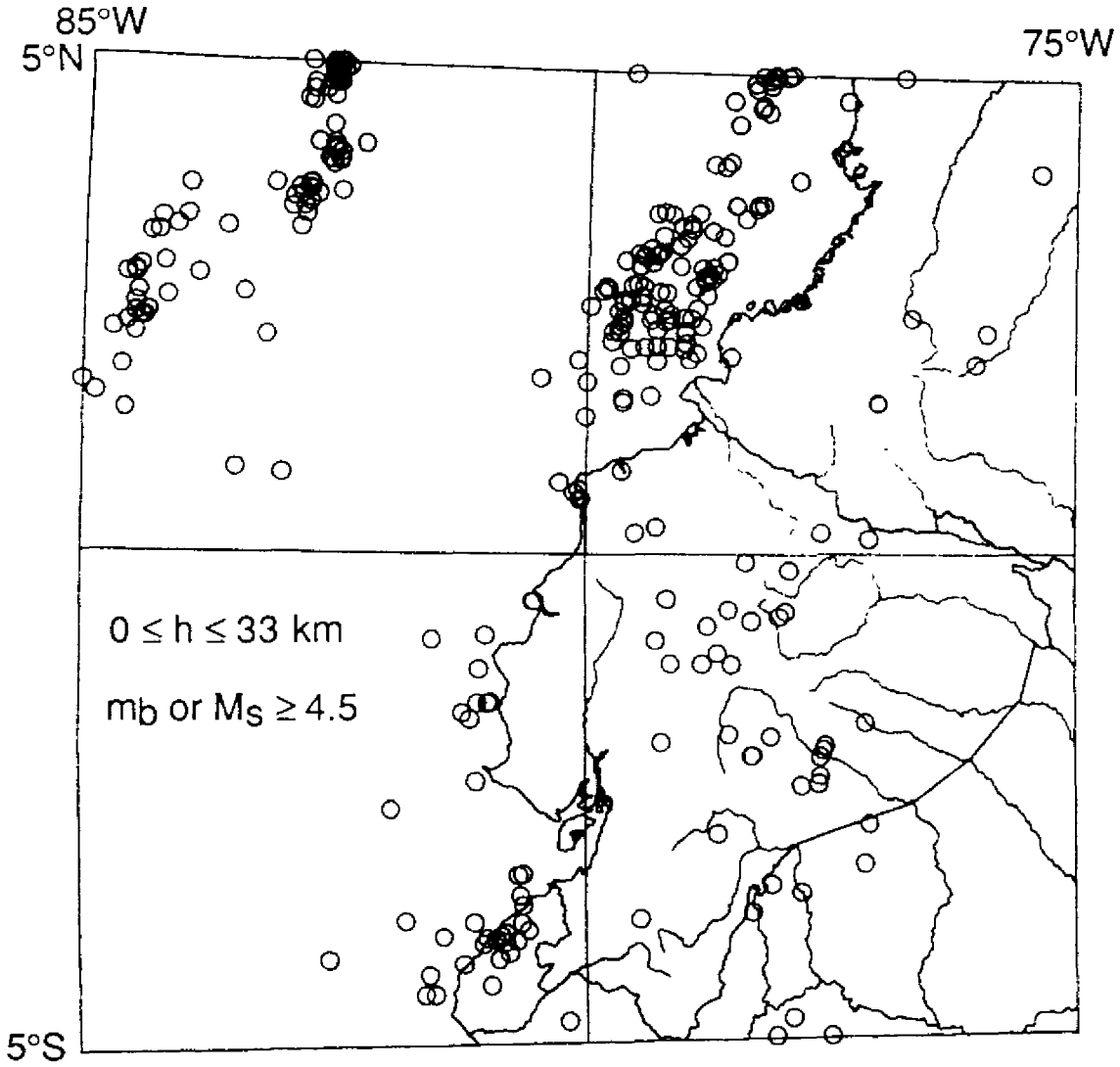

FIGURE 3.3A

FIGURES 3.3 Seismicity for the region of latitude 5°N to 5°S, longitude 75 to 85°W, for the period 1962 to 1987, inclusive. Map projection Oblique Mercator. Epicenters shown have been determined using 10 or more stations for earthquakes with magnitudes (m_b or M_s) equal to or greater than 4.5, and for (A) depth of focus, *h*, from surface to *h* equal to or less than 33 km; (B) for *h* greater than 33 km to *h* less than or equal to 100 km; and (C) for *h* greater than 100 km to *h* less than or equal to 300 km.

Studies of earthquake potential, using conditional probability estimates (Nishenko, 1989), have shown a 66 percent probability for a great earthquake (M_s > 7.7) to take place along the subduction zone between latitude 0.5°S and 1.2°N in the recurrence period of 1989-1999. The last large earthquake along this subduction zone occurred on May 14, 1942, with a surface-wave magnitude of 7.9. The conditional probability estimates were evaluated using the historical and instrumental seismicity catalogue of the

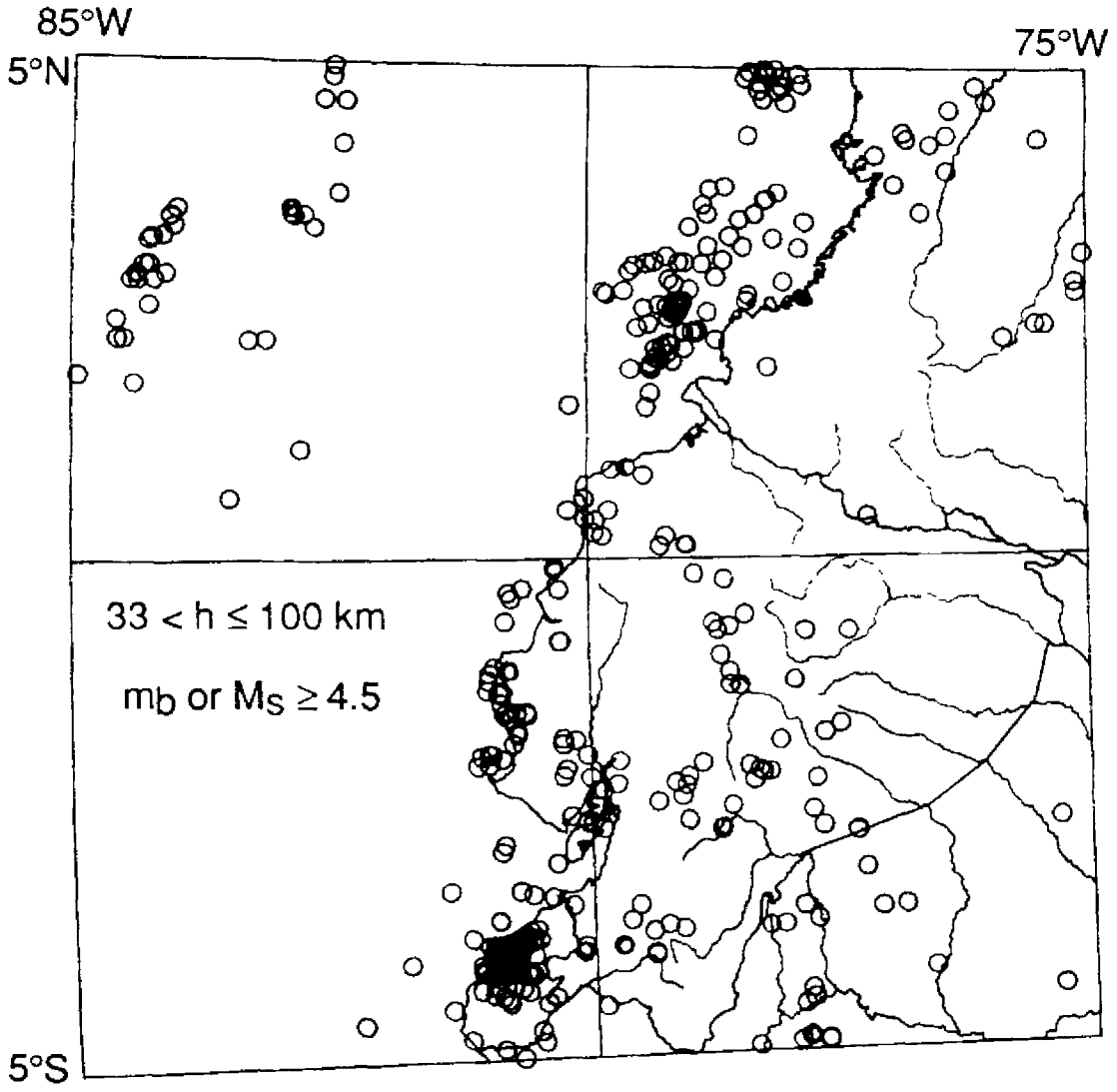

FIGURE 3.3B

region, although the historical record is poor for this region (Heaton and Hartzell, 1986).

The epicenters and magnitudes for the foreshock and the main event of March 5, 1987, determined by the U.S. Geological Survey, National Earthquake Information Center (NEIC), soon after the events, are presented in Table 3.1. These parameters were used to determine the focal mechanism solutions for these earthquakes. The seismic moment (M_o) for the foreshock was 5 x 10^{26} dyne-cm, and for the main event was 6.4 x 10^{26} dyne-cm. The above epicenters later were recalculated by the NEIC; the new earthquake parameters are given in Table 3.2.

The locations for the main foreshock, the main event, and the aftershocks were determined using the local network of stations deployed and maintained

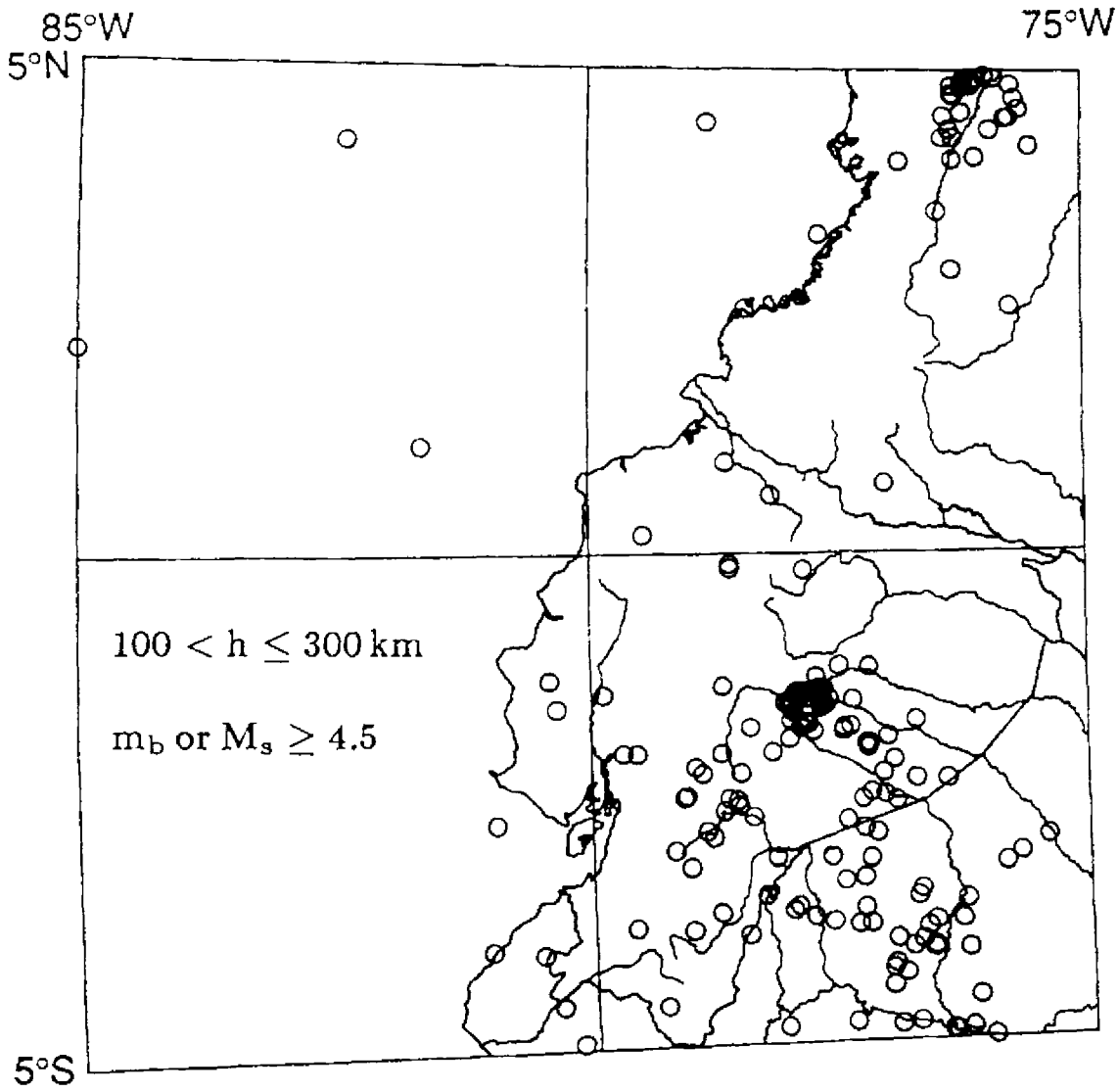

FIGURE 3.3C

by the Instituto Geofísico of the Escuela Politécnica Nacional, Quito; their earthquake parameter determinations are presented in Table 3.3.

Figure 3.2 shows the epicenters of the March 5 earthquakes listed in Table 3.1 as solid stars; their relocated epicenters, as listed in Table 3.2, as

TABLE 3.1 Initial Earthquake Parameters Calculated by U.S. Geological Survey

Date	Time	Lat.	Long.	Depth (km)	No. Obs.	M_s	m_b
5 March 1987	19:54	0.070°N	77.640°W	11	557	6.1	6.1
5 March 1987	22:10	0.120°N	77.800°W	13	594	6.9	6.4

TABLE 3.2 Revised Earthquake Parameters Calculated by U.S. Geological Survey

Date	Time	Lat.	Long.	Depth (km)	No. Obs.	M_s	m_b
5 March 1987	19:54	0.048°N	77.653°W	14	354	6.1	6.1
5 March 1987	22:10	0.151°N	77.821°W	10	344	6.9	6.5

TABLE 3.3 Earthquake Parameters Calculated by the Instituto Geofísico of the Escuela Politécnica Nacional

Date	Time	Lat.	Long.	Depth (km)
5 March 1987	19:54	0.142°S	77.871°W	3
5 March 1987	22:10	0.087°S	77.841°W	12

open stars; and their relation to the regional geology and principal fault systems around the epicentral region.

In Figure 3.4 are shown the number of aftershocks as a function of time following the 19:54 foreshock of the March 5 earthquake. As can be seen, the seismic activity decreased rapidly during the first 38 hr. The number of

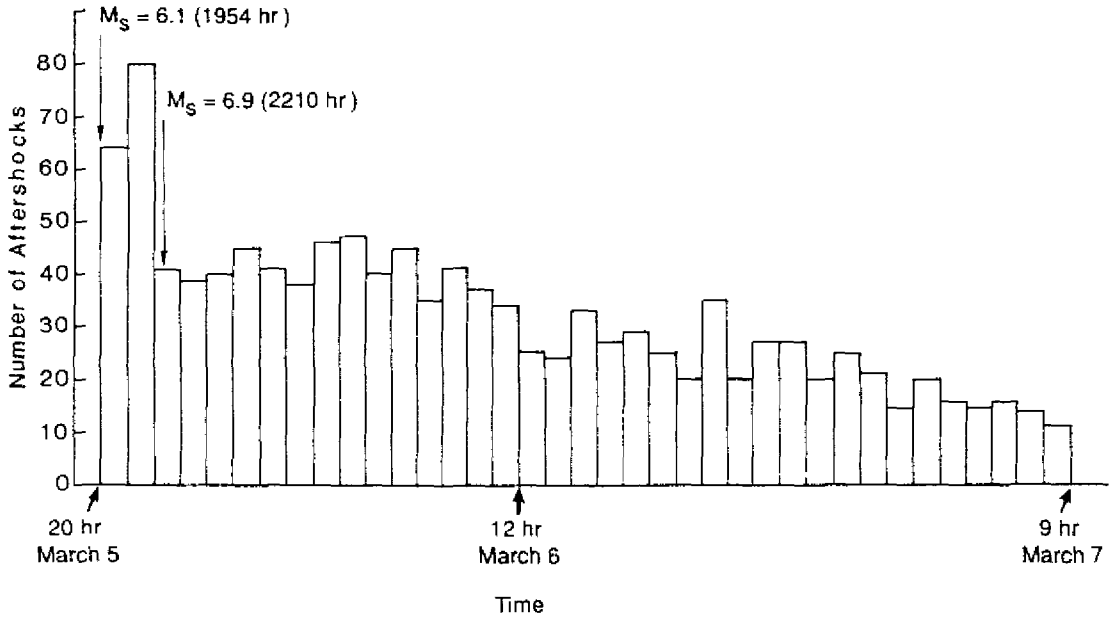

FIGURE 3.4 Number of aftershocks per hr recorded by a field seismological survey from the onset of the March 5, 1987, earthquakes through the first 38 hr. Total number of aftershocks was 1,240.

aftershocks per hr, immediately after the foreshock, was about 64 events, which increased to nearly 80 events before the main earthquake, and then decreased to an average of 40 events per hr during the next 14 hr. The number of events diminished to an average of 30 per hr during the subsequent 13 hr, and further decreased to an average of 15 events per hr during the next 18 hr. The total number of aftershocks in this 38-hr time lapse was 1,240. Relocations were done for 36 aftershocks that occurred between 19:54 and 22:10 on March 5 and for which the *S*-arrival times could be clearly read. The first group of 19 aftershocks, which occurred between 20:11 and 20:56, fall very tightly on a line with a NW direction, N 49° W. This trend is parallel to the lineament of the Salado River, shown in Figure 3.1. These aftershocks occurred in the region that sustained the highest degree of damage to the environment and to man-made structures. However, the second group of 17 aftershocks, which occurred between 20:57 and 22:03, do not correlate with any of the known faults in the region; however, their epicentral locations are dispersed throughout the meizoseismal area and do not

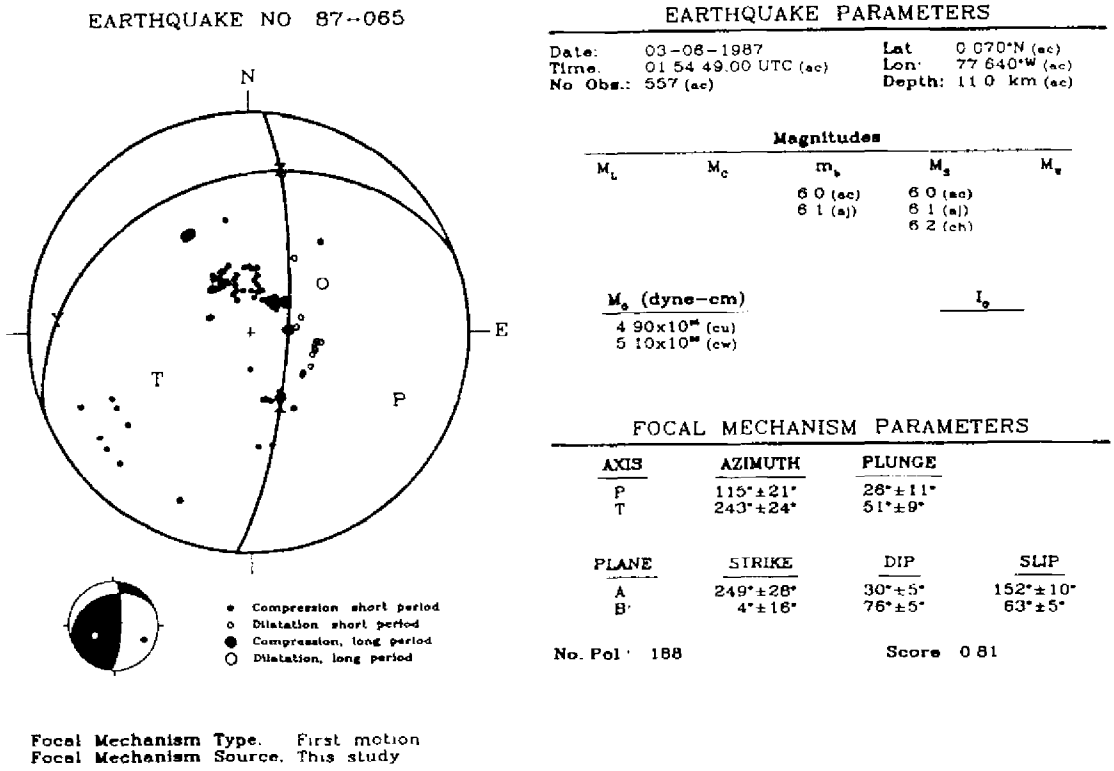

FIGURE 3.5 Focal-mechanism solution for the March 5, 1987, Ecuador earthquakes, with M_s = 6.1, using 188 *P*-wave observations. The magnitude and seismic moment are listed as obtained by different investigators. The earthquake parameters are the same as those listed in Table 3.1. Under the heading focal-mechanism parameters, the *P*- and *T*-axes and the fault planes A and B, Table 3.4, are given, and the uncertainty for each parameter is listed.

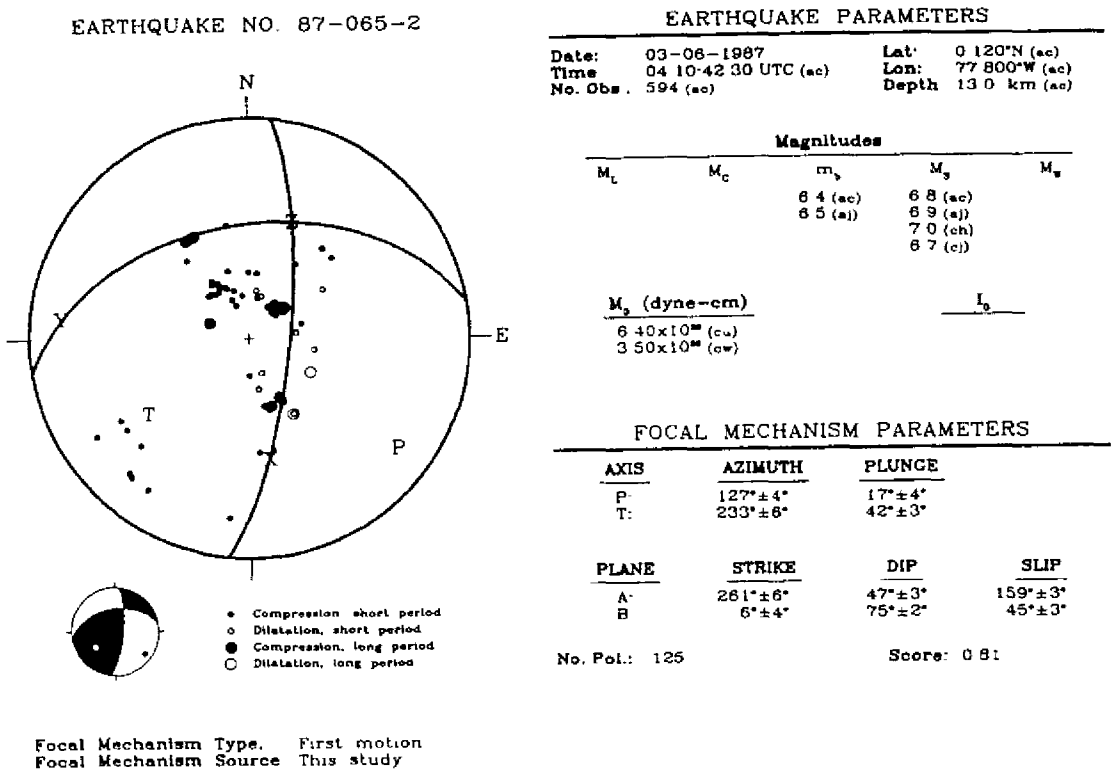

FIGURE 3.6 Focal-mechanism solution for the March 5, 1987, Ecuador earthquakes, with M_s = 6.1, using 125 *P*-wave observations. The magnitude and seismic moment are listed as obtained by different investigators. The earthquake parameters are the same as those listed in Table 3.1. Under focal-mechanism parameters, the *P*- and *T*-axes and the fault planes A and B, Table 3.4, are given, and the uncertainty for each parameter is listed.

follow any geologic or tectonic trend. No attempt was made to obtain joint focal-mechanism solutions from the observed aftershocks.

Focal-mechanism solutions obtained from first-motion studies for the foreshock and the main earthquake are shown in Figures 3.5 and 3.6. Table 3.4 lists the fault-plane solutions for these earthquakes. The March 5, 1987, 19:54 and 22:10 earthquakes have very similar focal-mechanism solutions. The uncertainty of each of the focal-mechanism parameters is given in

TABLE 3.4 Earthquake source parameters

	Plane A			Plane B			
EQ. #	Strike	Dip	Slip	Strike	Dip	Slip	No. of Obs.
1	N 69° E	30°W	152°	N 4° E	76°E	63°	188
2	N 81° E	47°W	159°	N 6° E	75°E	45°	125

Figures 3.5 and 3.6. For the main event, the number of polarizations used was 125 and the solution is very stable. The uncertainties in the parameters for the focal-mechanism solution of the foreshock are slightly greater than for the main event. The solutions presented in Figures 3.5 and 3.6 exhibit good correlation with the regional faults shown in Figure 3.2.

The focal-mechanism solutions, shown in Figures 3.5 and 3.6 represent a point-source solution and hence do not represent, in the near field, the finite structure of the rupture process (dislocation). As pointed out in the post-earthquake intensity-distribution study by Espinosa et al. (Chapter 4), the town of Olmedo (Figure 4.3), west of the epicenters of the foreshock and main event, sustained higher damage to the infrastructure than did other towns N or S of the epicenters. The isoseismals VI and VII (Figure 4.5 in Espinosa et al., Chapter 4) exhibit a preferential azimuthal distribution to the NW, which could indicate a directivity function due to a dislocation moving in this direction. A similar process, very well defined by the isoseismal distribution, was observed after the Guatemala earthquake of 1976 (Espinosa et al., 1976).

RECOMMENDATIONS

In view of the results we have obtained in the postearthquake field study, we believe there is an urgent need to evaluate the earthquake hazards in Ecuador. We recommend the following activities:

1. Compile a more extensive and detailed historical earthquake catalogue for interplate and intraplate earthquakes in Ecuador.
2. Compile a historical earthquake catalogue for events that are associated with volcanism.
3. Perform paleoseismicity studies in the NW part of Ecuador, especially in the region of Jama (latitude 0.5°S to 1.2°N), in order to ascertain the past occurrence of large and/or great earthquakes in this high-earthquake-potential region.
4. Deploy sensitive seismological instruments in the region (latitude 0.5°S to 1.2°N) in order to ascertain the level of seismicity and to study the joint focal mechanisms.
5. Study the characteristics and ages of marine terraces in order to better understand the past occurrence of great earthquakes in the region.
6. Evaluate the mode of subduction and its geometry in the Wadati-Benioff zone under Ecuador, in order to create a 3-D lithospheric model and to map the maximum horizontal stress distribution in the plate. This task will assist in delineating regions with high earthquake potential.
7. Evaluate the focal-mechanism solutions for all large and great earthquakes in Ecuador.

8. Based upon the above results, outline a working model of the tectonic regime of the region.

REFERENCES

Egred, J. 1988. Terremoto de la Provincia del Napo, Marzo 5, 1987. Instituto Geofísico, Escuela Politécnica Nacional, Quito, Ecuador, 56.

Espinosa, A. F. 1979. Geologic hazards. Pp. 119–144 in Energy Resources of Peru. U.S. Geological Survey Project Report: Peru Investigations (IR) PE-6.

Espinosa, A. F., R. Husid, and A. Quesada. 1976. Intensity distribution and source parameters from field observations of the February 4, 1976, Guatemalan earthquake. Pp. 52–66 in The Guatemalan Earthquake of February 4, 1976, a Preliminary Report. A. F. Espinosa, ed. U.S. Geological Survey Professional Paper 1002.

Hall, M., and C. Wood. 1985. Volcano-tectonic segmentation of the northern Andes. Geology 13:203–207.

Heaton, T. H., and S. H. Hartzell. 1986. Source characteristics of hypothetical subduction earthquakes in the northwestern United States. Bulletin of the Seismological Society of America 76:675–708.

Kanamori, H., and K. C. McNally. 1982. Variable rupture mode of the subduction zone along the Ecuador-Colombia coast. Bulletin of the Seismological Society of America 72:1241–1253.

Lonsdale, P. 1978. Ecuadorian subduction system. American Association of Petroleum Geologists Bulletin 89:981–999.

Lonsdale, P., and K. Klitgard. 1978. Structure and tectonic history of the Eastern Panama Basin. Geological Society of America Bulletin 89:981–999.

Nishenko, S. P. 1989. Circum-Pacific Seismic Potential, 1989-1999. U.S. Geological Survey Open-File Report 89-86:126.

Pennington, W. 1981. Subduction of the Eastern Panama Basin and seismotectonics of northwestern South America. Journal of Geophysical Research 86:10753–10770.

Pilger, R. 1983. Kinematics of the South American subduction zone from global plate reconstructions. American Geophysical Union, Geodynamics Series 11:113–125.